J. Biochem. **136**, 57–64 (2004)
DOI: 10.1093/jb/mvh095

Interaction of Myosin·ADP·Fluorometal Complexes with Fluorescent Probes and Direct Observation Using Quick-Freeze Deep-Etch Electron Microscopy

Shinsaku Maruta[1,*], Yasuo Uyehara[1], Tomoki Aihara[1] and Eisaku Katayama[2]

[1]Department of Bioengineering, Soka University, Hachioji, Tokyo 192-8577; [2]Division Biomolecular Imaging, Institute of Medical Science, University of Tokyo, Minato-Ku, Tokyo 108-8639; and PREST, JSP, Kawaguchi, Saitama

Received January 20, 2004; accepted April 26, 2004

Myosin forms stable ternary complexes with ADP and phosphate analogues of fluorometals that mimic different ATPase reaction intermediates corresponding to each step of the cross-bridge cycle. In the present study, we monitored the formation of ternary complexes of myosin·ADP·fluorometal using the fluorescence probe prodan. It has been reported that the fluorescence changes of the probe reflect the formation of intermediates in the ATPase reaction [Hiratsuka (1998) *Biochemistry* 37, 7167–7176]. Prodan bound to skeletal muscle heavy-mero-myosin (HMM)·ADP·fluorometal, with each complex showing different fluorescence spectra. Prodan bound to the HMM·ADP·BeFn complex showed a slightly smaller red-shift than other complexes in the presence of ATP, suggesting a difference in the localized conformation or a difference in the population of BeFn species of global shape. We also examined directly the global structure of the HMM·ADP·fluorometal complexes using quick-freeze deep-etch replica electron microscopy. The HMM heads in the absence of nucleotides were mostly straight and elongated. In contrast, the HMM heads of ternary complexes showed sharply kinked or rounded configurations as seen in the presence of ATP. This is the first report of the direct observation of myosin-ADP-fluorometal ternary complexes, and the results suggest that these complexes indeed mimic the shape of the myosin head during ATP hydrolysis.

Key words: conformational change, electron microscopy, energy transduction, fluorescence probe, myosin.

Abbreviations: AlF_4^-, aluminum fluoride; BeFn, beryllium fluoride; DTT, dithiothreitol; GaFn, gallium fluoride; HMM, heavy-mero-myosin; MgFn, magnesium fluoride; S-1, myosin subfragment-1; S-1Dc, myosin head from *Dictyostelium discoideum* myosin II; SDS-PAGE, sodium dodecyl sulphate polyacrylamide gel electrophoresis;Vi, vanadate.

Muscle contraction is based on the interaction between myosin and actin coupled with ATP hydrolysis. Myosin hydrolyzes ATP via several steps in its kinetic pathway. Numerous biochemical studies have demonstrated that ATP hydrolysis and the formation of intermediates is accompanied by localized changes in the conformation of the myosin head, *e.g.* in the regions of Trp 510 (*1–3*), Cys 707-Cys 697 (*4–6*) and Lys 83 (*7–9*). Furthermore, global morphological changes in the myosin head during ATP hydrolysis have also been demonstrated using small angle synchrotron x-ray scattering (*10*, *11*). The sequence of transient intermediates on the kinetic pathway may represent changes in the conformation of localized regions and the global shape. However, it is often difficult to study the sequence of such changes due to the brief lifetime of the transient intermediates. Consequently, the precise nature of the conformational changes in the myosin head that are directly related to energy transduction remain unclear. To study conformational changes in transient intermediates in the ATPase cycle and their roles in energy transduction in detail, the use of stable analogues mimicking the structures of the intermediates would be very useful.

In the presence of Mg^{2+}-ADP, myosin forms stable ternary complexes with phosphate analogues, beryllium fluoride (BeFn) (*12–14*), vanadate (Vi) (*15*), aluminum fluoride (AlF_4^-) (*12*, *13*) and scandium fluoride (ScFn) (*16*). Solution studies using fluorescence, CD, NMR, and EPR techniques have demonstrated differences in the structure of various stable myosin-ADP-phosphate analogue complexes. Furthermore, crystallographic studies of complexes of recombinant truncated *Dictyostelium*-S1 (S1Dc)·ADP·AlF_4^-, S1Dc·ADP·BeFn (*17*, *18*) and S1Dc·ADP·Vi (*19*) have also shown significant structural differences between the complexes and indicated that these ternary complexes may mimic different transient states along the ATPase kinetic pathway; myosin·ADP·AlF_4^- and myosin·ADP·Vi complexes resemble the M^{**}·ADP·Pi intermediate state while myosin·ADP·BeFn mimics the M^{*}·ADP·Pi state.

Crystallographic studies have shown the exact three-dimensional coordination of amino acids of the myosin

*To whom correspondence should be addressed.:A/Prof. Shinsaku Maruta, Department of Bioengineering, Faculty of Engineering, Soka University, Phone: +81-426-91-9443, Fax: +81-426-91-9312, E-mail: shinsaku@t.soka.ac.jp

motor domain, and provide useful information regarding the possible mechanisms of energy transduction. However, discrepancies among numerous biochemical data, especially with respect to conformational changes at the flexible regions of myosin, suggest that the crystal structures may not reflect the actual conformation of myosin in solution. For instance, the Vi or AlF_4^- complexes are thought to correspond to the M**·ADP·Pi state; yet their crystal structures suggest that the cysteine region forms a helix, and, therefore, that the distance between reactive cysteine residues, Cys 707 and Cys 697, is identical to that of non-nucleotide myosin (*18*, *19*). Cross-linking experiments have revealed that the distance between Cys 707 and Cys 697 is reduced from 12–14 Å to 3–5 Å during ATP hydrolysis (*5*, *6*). With respect to the BeFn complex, an analysis of tryptophan fluorescence enhancement as well as its interaction with actin indicates that it is different from the non-nucleotide state (*12–14*).

The most likely constitutively flexible regions of the methylated skeletal muscle myosin head are loops 204–216 and 627–646, located at the junctions of the 25 and 50 kDa fragments and the 50 and 20 kDa fragments, respectively, but the loops cannot be seen in crystal structures (*20*). X-ray solution scattering of ternary complexes has suggested that all such complexes, including the BeFn complex, have a compact or round myosin head as seen in the presence of ATP (*10*, *21*). Furthermore, recent crystallographic studies of smooth muscle myosin-ADP-fluorometal complexes demonstrated that both BeFn and AlF_4^- complexes have morphologically similar regulatory domains that resemble the M**·ADP·Pi state (*22*). However, the results of studies comparing the structures of skeletal muscle myosin are confusing, particularly with respect to the sequential conformational changes along the ATPase cycle. Only for scallop myosin, the crystal structures corresponding to different three states of a single isoform have been reported by Houdusse et al. (*23*, *24*) These structures show that the first conformation of scallop S-1 in the absence of nucleotide is similar to that of chicken skeletal myosin, and the second conformation in the presence of ADP·Vi is similar to that of chicken smooth muscle myosin. And, interestingly, the third conformation of scallop S-1 in the presence of ADP shows an unusual conformation of the myosin head: the converter and the lever arm are in quite different positions from those in either the pre-power stroke or near-rigor state structure. Moreover, in contrast to these structures, it has been shown that the SH1 helix is unwound. The unusual structure has been suggested to represent one of the prehydrolysis ("ATP") states of weak actin-binding but not a strong actin-binding "ADP" state. Thus the crystal structure remains in conflict with the structures in solution.

6-Propionyl-2- (dimethylamino) naphthalene (prodan), a fluorescent probe, is widely used as a sensitive reporter for hydrophobic protein sites. The probe has been applied successfully to the study of apomyoglobin (*25*), tubulin (*26*), and spectrin (*27*). Hiratsuka (*28*) applied the probe for myosin and succeeded in isolating S-1 in the S-1**·ADP·Pi state from other forms in free and S1*·ADP states and continuously visualizing the ATPase reaction (*28*). The same probe was used in the present study to monitor the conformational changes in the myosin head associated with the formation of myosin·ADP·fluorometal ternary complexes and to characterize the precise differences between the BeFn complex and other complexes.

We also employed quick freeze deep-etch replica electron microscopy to examine directly morphological changes in the myosin head during the formation of ternary complexes with ADP and fluorometal phosphate analogues. This technique, coupled with pre-adsorption of the sample onto the surface of mica-flakes, has been used by Heuser (*29*) for visualizing macromolecules. Katayama (*30*) used the same technique and demonstrated that the actin structure comprises a ring-shaped particle with one or two clefts across the rim giving rise to a horseshoe-like appearance. Moreover, Katayama (*30*) also noted that the actin-unbound HMM-head is generally straight and elongated in the absence of nucleotides, whereas upon the addition of ATP or ADP/Vi to the solution, it kinks sharply so that the two head moieties connected to each other appear sigmoidal in shape (*30*). Thus, quick freeze deep-etch replica electron microscopy is very useful for direct examination of the structure of the myosin head in solution, where it assumes different transient states in the ATPase cycle. To our knowledge, this is the first study involving the direct visualization of myosin·ADP·fluorometal ternary complexes using the technique of quick freeze deep-etch replica electron microscopy.

MATERIALS AND METHODS

Protein Preparations—Myosin was prepared from chicken breast muscle according to the method of Perry (*31*). The isolated myosin was then digested with α-chymotrypsin to obtain subfragment-1 (S-1) as described by Weeds and Taylor (*32*). HMM was prepared according to the method of Weeds and Pope (*33*).

Chemicals—ATP, ADP, dithiothreitol, Tris, NaF, $BeSO_4$, and sodium orthovanadate were purchased from Wako Pure Chemicals (Wako, Osaka, Japan). $AlCl_3$, $ScCl_3$, $GaCl_3$ were purchased from Aldrich. Prodan was purchased from Molecular Probes Inc. (Eugene, OR).

Quick-Freezing for Electron Microscopy—HMM·ADP·AlF_4^-, HMM-ADP-BeFn and HMM-ADP-Vi ternary complexes were prepared according to the method of Maruta et al. (*12*). Briefly, 10 μg/ml HMM was incubated with 1 mM ADP and 1 mM AlF4-, BeFn or Vi in a solution containing 120 mM NaCl, 50 mM ammonium acetate, and 5 mM $MgCl_2$ for 2 h at 25°C. The HMM-ADP-GaFn complex was prepared as described previously by our laboratory (*21*). Briefly, 10 μg/ml HMM was incubated with 1 mM ADP and 0.1 mM GaFn in a solution containing 120 mM NaCl, 50 mM ammonium acetate, and 5 mM $MgCl_2$ for 2 hrs at 25°C. The HMM-ADP-fluorometal complexes were diluted to 10–15 μg/ml about two minutes before the quick freezing procedure. The diluted samples of HMM-ADP-fluorometals ternary complex samples were adsorbed onto mica flakes before freezing, and then subjected to the same procedure. Mica flakes are very effective as a spacer material to maintain low viscosity samples in a solid form. The suspension of mica adsorbed samples was frozen quickly by contact with a pure copper block (Polaron E-7200) cooled to liquid helium temperature (*34*). Quick-frozen HMM were set in a Baltzer's type

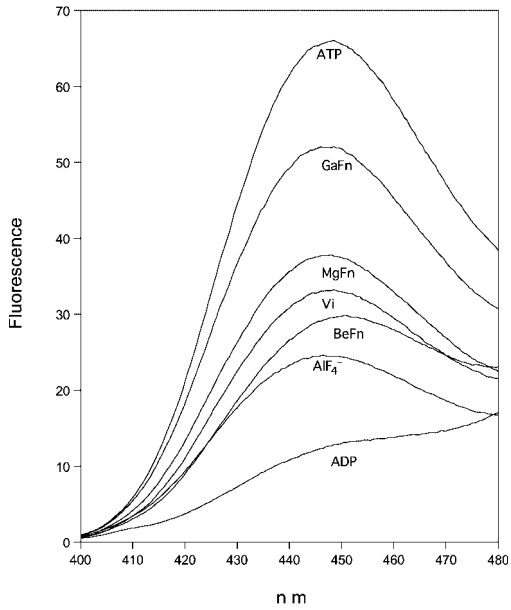

Fig. 1. **Changes in the fluorescence emission spectrum of the prodan·S-1 complex induced by ATP, ADP and ADP·fluorometals.** Fluorescence spectra of the complex of 20 μM S-1 with 4 μM prodan were recorded in the presence of 1 mM ATP, 1 mM ADP and ADP·Pi analogues, 1 mM ADP + 1 mM AlF_4^-, BeFn, Vi, 0.1 mM GaFn or 5 mM MgFn. The buffer condition: 120 mM NaCl, 30 mM Tris-HCl pH7.5, 2 mM $MgCl_2$.

300 machine and fractured, etched for 4 min at –104°C and rotary shadowed with platinum at an angle of 6°. Carbon coated specimens were floated on water and residual mica flakes were dissolved overnight on the surface of full strength hydrofluoric acid. Replicas were picked up and stereo pictures were taken.

Fluorescence Measurement—Fluorescence measurements were obtained at 25°C with an RF-500 Spectrofluorometer (Shimadzu, Japan).

RESULTS

Fluorescence Studies of HMM-ADP-Fluorometal Complexes Using the Fluorescent Probe Prodan—Hiratsuka (*28*) demonstrated that the fluorescent probe prodan binds to S-1 stoichiometrically without affecting the enzymatic properties (ATPase and actin binding) of S-1. The emission peak at 460 nm of prodan bound to rabbit skeletal S-1 shifts to 450 nm and 445 nm upon the addition of ADP and ATP, respectively, indicating that the spectral changes reflect the different transient states, M^*·ADP and M^{**}·ADP·Pi, in ATPase cycle. Similar spectral changes were noted between chicken skeletal S-1 and rabbit skeletal S-1 (Fig. 1). Interestingly, no changes in the fluorescent spectra were noted when smooth muscle S-1 was used (data not shown). This may be due to the structural differences between skeletal and smooth myosin as shown in recent crystal structures. Therefore, prodan seems to be specific for skeletal muscle myosin and is useful for monitoring the formation of transient states in the ATPase cycle.

In the next series of studies, we determined the fluorescence spectra of prodan bound to S1·ADP·fluorometal complexes. These spectra were then compared with those in the presence of ADP and ATP. Upon the addition of excess ATP (1 mM) or ADP (1 mM), the emission maximum at 460 nm blue-shifted further to 448 nm or 453 nm, respectively. As shown in Fig. 1, the fluorescence spectra of prodan·S-1 complexes in the presence of ADP·fluorometals also further blue-shifted due to the formation of prodan·S-1·ADP·fluorometal complexes. However, slight differences in the spectra were noted among the complexes, which might reflect conformational differences in prodan binding to a localized region of the myosin head. The peak emission of the prodan·S-1·ADP·BeFn complex red-shifted to 451 nm, more than other complexes. Other complexes, with the exception of the BeFn complex, showed emission maximam at 448 nm, similar to that in the presence of ATP. These results suggest that prodan bound to ternary complexes allows the detection of differences in the detailed conformations, which may be explained by different transient states in the ATPase cycle around at the M^{**}·ADP·Pi state.

Examination of HMM-ADP-Fluorometal Ternary Complexes by Quick-Freeze Deep-Etch Electron Microscopy—Using quick freeze deep etch electron microscopy, Katayama (*30*) demonstrated free HMM kinks in the presence of ATP so that the two head moieties connected to each other appear sigmoidal in shape, whereas in the absence of ATP, the HMM head is generally straight and elongated as illustrated in Figure 3A. We used the same technique to examine directly the shape of HMM heads during the formation of ternary complexes with ADP and fluorometals. As a control, we also observed HMM in the presence of ATP, ADP and in the absence of nucleotides under the same conditions. Figure 2a and c show HMM particles in the absence of ATP and presence of ADP, respectively. The HMM heads appear elongated and mostly straight or only slightly curved with a conventional pear-shaped morphology. In the presence of ATP, the majority of HMM changed to a sharply kinked configuration, forming a sigmoid (Fig. 2b) as reported previously (*30*).

HMM·ADP·fluorometal ternary complexes were prepared and diluted a few minutes before quick freezing for deep etch electron microscopy. The formation of ternary complexes after dilution was confirmed functionally by measuring the loss of ATPase activity (data not shown). The results showed that the formation of ternary complexes is associated with more than 90% inhibition. The configuration of the HMM·ADP·AlF_4^- ternary complex, an analogue of the M^{**}·ADP·Pi state, is almost identical to that in the presence of ATP (Fig. 2d). Almost all heads formed ternary complexes with ADP and AlF_4^- under our experimental conditions and all showed kinked configurations. These results are consistent with small angle X-ray scattering measurements of the myosin S1·ADP·AlF_4^- ternary complex; the profiles of scattering angle-intensity relationship indicate that the S-1 heads form a ternary complex bend (*11*).

Interestingly, the HMM·ADP·BeFn ternary complex, which is considered to be an analogue of the M^*·ATP state, also showed a sharp kinked configuration. These results are inconsistent with the crystallographic observation of the truncated Dictyostelium-S1·ADP·BeFn complex, which resembles the straight shape noted in the absence of nucleotide (*18*). We also examined the HMM·

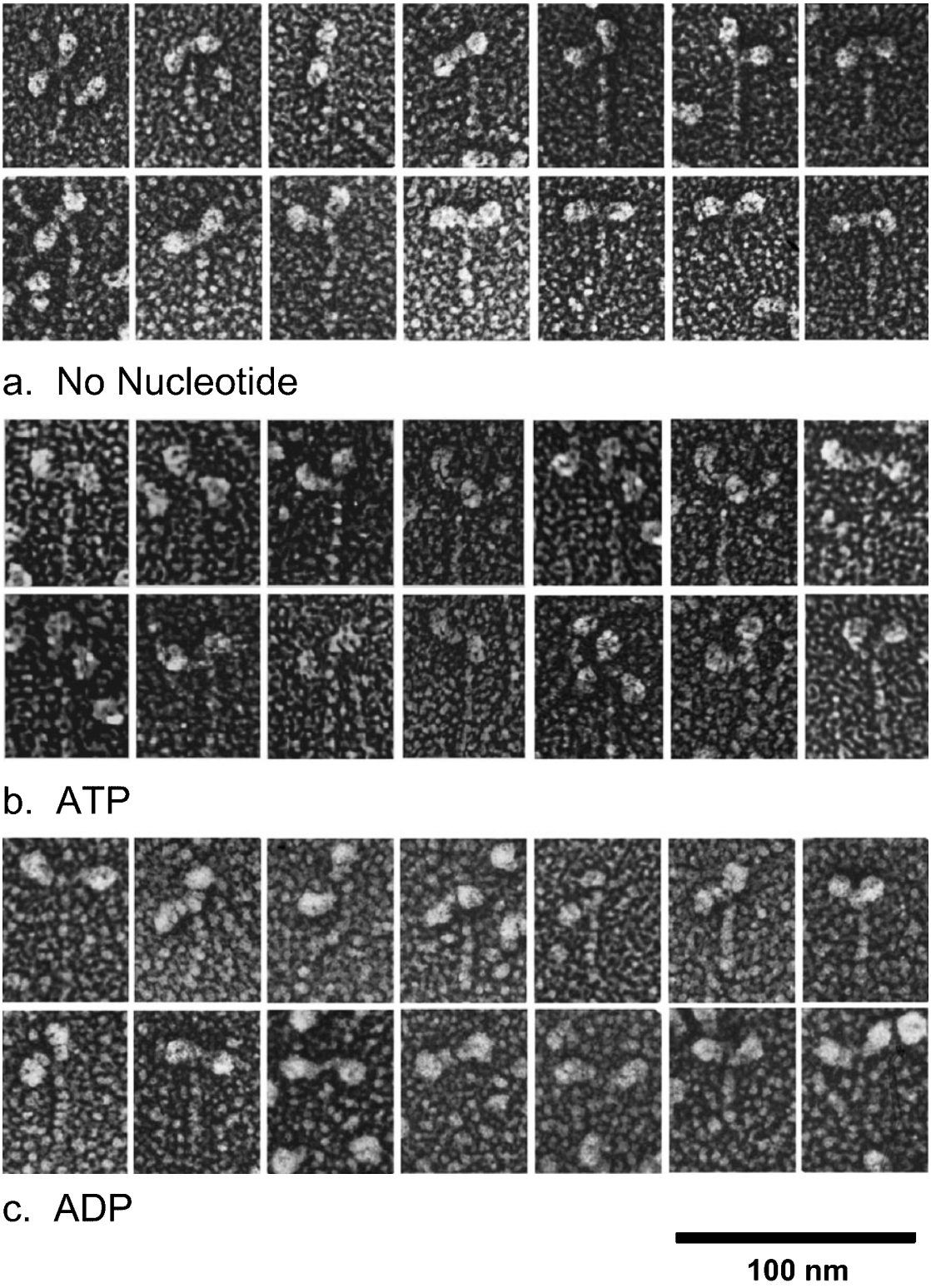

Fig. 2. (a–c)

ADP·Vi complex and demonstrated that the complex has a kinked configuration, as reported previously by Katayama (*30*). We have classified the shapes observed by electron microscopy into three types: [1] straight, [2] rounded or slightly kinked, and [3] kinked and sigmoidal as shown in Fig 3A. [1] Straight heads are approximately 20 nm long and 10 nm wide. [2] Rounded or slightly kinked heads are shorter and wider than straight heads, and are slightly kinked without a sigmoidal configuration of the two heads. [3] Kinked and sigmoidal heads are strongly kinked at a bending angle of 50–90 degrees with a sigmoidal configuration of the two heads. The shapes have been statistically analyzed as shown in Fig. 3B. For the HMM·ADP·Pi analogue complexes, the proportion of

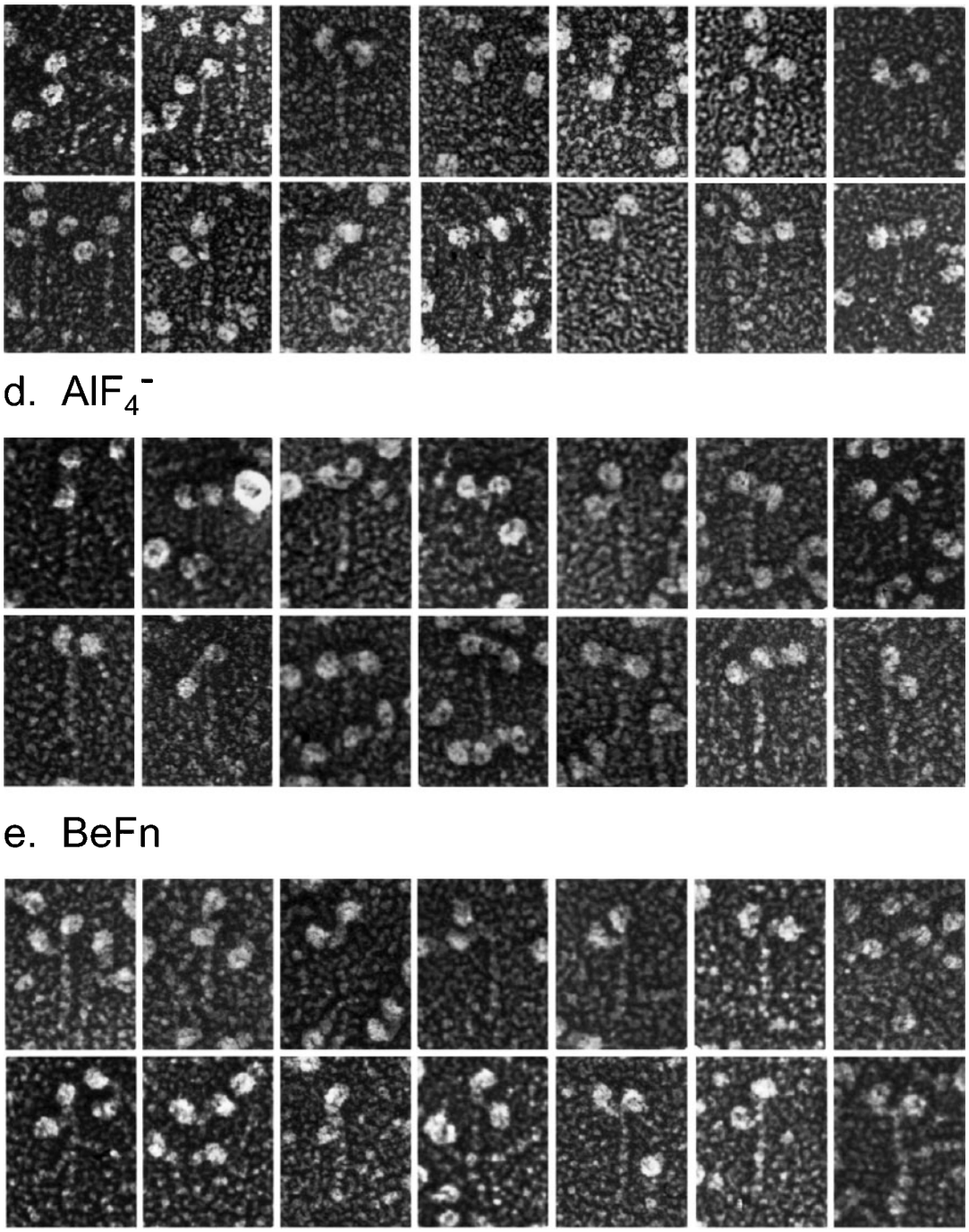

Fig. 2. **Gallery of typical HMM conformers in the presence of ADP and Pi analogues.** (a) HMM molecules in the absence of nucleotide, (b) in the presence of ATP, (c) in the presence of ADP (d) HMM·ADP·AlF_4^-, (e) HMM·ADP·BeFn, (f) HMM·ADP·Vi

the straight shape dramatically decreases and mostly kinked and rounded shapes are observed. In the presence of ATP, the strongly kinked and sigmoidal shape is more prominent than ternary complexes.We also examined the recently characterized ternary complexes of HMM·ADP·GaFn and HMM·ADP·MgFn, both of which are considered to be M^{**}·ADP·Pi analogues. As expected from the biochemical experiments, both complexes showed kinked configurations similar to other ternary complexes, confirming that they mimic the M^{**}·ADP·Pi state.

DISCUSSION

Determination of the serial changes in conformation of the myosin motor domain that accompany the formation of transient intermediates during the progression of the

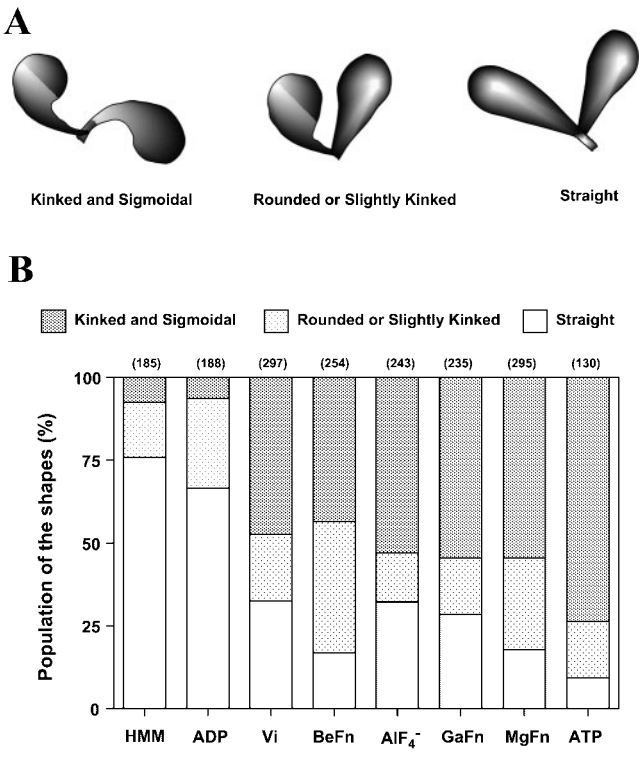

Fig. 3. **A: Schematic representation of the shapes of HMM·ADP·Pi analogue ternary complexes based on the electron micrographs.** The shape of the myosin head was classified into three types, straight, rounded or slightly kinked, and kinked and sigmoidal. **B: Ratios of the different shapes of the myosin head among HMM·ADP·Pi ternary complexes.** The shapes of the heads were statistically analyzed. (1) Straight heads are approximately 20 nm long and 10 nm wide. (2) Rounded or slightly kinked heads are shorter and wider than the straight heads, and slightly kinked without a sigmoidal configuration of the two heads. (3) Kinked and sigmoidal heads are strongly kinked at a bending angle of 50–90 degrees with a sigmoidal configuration of the two heads. The numbers in the parenthesis indicate the number of samples analyzed.

ATPase cycle is important for understanding the structural basis of force generation. The use of stable myosin·ADP·Pi analogue ternary complexes that mimic various transient intermediates in the ATPase cycle would be very useful in studies designed to investigate the mechanism of energy transduction.It has been previously demonstrated that in the presence of Mg^{2+}-ADP, myosin forms stable ternary complexes with Pi analogue of fluorometals, AlF_4^-, BeFn, ScFn, GaFn and MgFn, and that the ternary complexes mimic different transient states along the steady state in the ATPase cycle (*12*, *16*, *21*, *37*). Subsequently, recent crystallographic studies showed that smooth muscle S-1 forms ternary complexes with ADP and fluorometals, which mimic transient states along the ATPase cycle, with sharp kinks at the junction of the motor and regulatory domains (*22*). However, significant differences among the ternary complexes, except the BeFn complex, have not yet been detected.

The important thing for the application of these complexes to the kinetic studies is that the ternary complexes each mimic different distinguishable steps distributed widely along the myosin ATPase kinetic pathway. In the present study, we show that these complexes each show apparently different states when examined using the fluorescent probe prodan.Previously, Hiratsuka has demonstrated that the fluorescence of prodan reflects the conformational change in the motor domain in ATPase cycle (*28*).As shown in Fig. 1, ternary complexes show apparently different fluorescence spectra, indicating that these complexes have different conformations. A number of previous studies have suggested that S1·ADP·BeFn mimics the M^*·ATP state, while other complexes (AlF_4^-, Vi, ScFn, GaFn, and MgFn) mimic the M^{**}·ADP·Pi state.

However, these ternary complexes may not resemble exactly the M^*·ATP or M^{**}·ADP·Pi state, but mimic slightly different structures that are observed in transient states from the M to the M^{**}·ADP·Pi state. We have previously suggested a possible alignment of the ternary complexes mimicking the transient intermediates in ATPase cycle as follows (*21*):

$$\begin{matrix} {}^*\text{BeFn} & {}^{**}\text{BeFn} & \text{MgFn} & \begin{matrix}(\text{ScFn})\\ \text{AlF}_4^-\end{matrix} \\ \text{M}^*\cdot\text{ATP} & \rightarrow \text{M}^{**}\cdot\text{ADP}\cdot\text{Pi} & \rightarrow \text{M}^*\cdot\text{ADP} & \end{matrix}$$

The differences in the spectra of prodan bound to the ternary complexes strongly support the idea that the complexes mimic transient intermediates from the M^* to M^{**} state.

Prodan specifically and sensitively reflects the conformational change in skeletal muscle myosin in the ATPase cycle resulting from monitoring the circumstances of the probe. Although we have applied prodan to smooth muscle myosin, the conformational change in the smooth muscle myosin head in the ATPase cycle was not detected from the fluorescence of prodan, because prodan does not bind to smooth muscle myosin sufficiently for its fluorescence to be measured. This suggests that the energy transducing site of smooth muscle myosin is different from that of skeletal muscle. This may also support the idea that the life time and stability of transient intermediates in the ATPase cycle of smooth muscle myosin differ somewhat from those of skeletal muscle myosin. In support of this idea, we have previously demonstrated that skeletal muscle myosin hydrolyzing 8-Br-ATP, which has a *Syn* conformation with respect to the N-glycoside bond, resembles the M^*·ATP state and does not support actin filament sliding. Contrary, smooth muscle myosin forms M^{**}·ADP·Pi state with 8-Br-ATP, enhances 20% intrinsic tryptophan fluorescence and supports actin sliding.

Although it is generally believed that the S-1·ADP·BeFn ternary complex resembles the M^*·ATP state based on a number of biochemical and crystallographic studies of the truncated Dictyostelium-S1 motor domain·ADP·BeFn complex (*8*, *39*), our previous studies indicated that the complex mimics the M^{**}·ADP·Pi state rather than the M^*·ATP state (*12*, *21*, *38*).

The discrepancy may be explained by our previous observation that BeFn exists in several forms in solution. Our ^{19}F-NMR studies demonstrated that, in solution, BeFn incorporated into ternary complexes exists as at least in four species (*38*). Moreover, the ^{19}F-NMR spectrum of a ^{19}F-labeled ADP analogue, trapped into SKE-S1 with BeFn, showed two distinct adenine moiety coordinates (*39*). It is proposed that BeFn species are distinct from each other with regard to their characteristics, and

that ternary complexes composed of these species may mimic different states in the ATPase cycle. Thus, one species may mimic the M^{**}·ADP·Pi state, while another may mimic the M^{*}·ATP state. The Dictyostelium-S1·ADP·BeFn crystal reported by Rayment et al. (*20*) might contain a species that mimics the M^{*}·ATP state under the preparation conditions. The fluorescence spectra of prodan·S1·ADP·BeFn complexes show emission peaks that are slightly red shifted as compared with other ternary complexes (Fig. 1), suggesting the possible presence of multiple BeFn species.

However, the data obtained by the methods described above reveal the average S-1 particles form ternary complexes, which may assume different shapes due to the different fluorometals, such as BeFn. We have employed a quick freeze deep etch replica electron microscopic method to observe directly individual particles of S-1·ADP·fluorometal ternary complexes. As shown in Fig. 2 and 3, all of the ternary complexes showed a predominantly kinked configuration. Statistical analysis of the shape of the ternary complexes indicated that the BeFn complex is more rounded and slightly kinked than the other complexes (Fig. 3). This clearly suggests the existence of several species of BeFn.

The findings from quick-freeze deep etch electron microscopy are consistent with our previous results obtained by X-ray small angle scattering measurement (*21*). The latter technique is useful for directly detecting large-scale changes in the molecular structures of various complexes in solution under physiological conditions. We have shown that ternary complexes, which exhibit a kinked configuration on quick-freeze deep etch electron microscopy, have smaller radius gyration values, suggesting that they become compact or round in shape, similar to what takes place in the presence of ATP.

In conclusion, we have demonstrated that the fluorescent probe, prodan is useful for monitoring the formation of myosin·ADP·fluorometal ternary complexes. The small conformational differences among the complexes are sensitively shown by the fluorescence spectra of prodan bound to the ternary complexes, reflecting conformational changes in the myosin head. Quick freeze deep etch replica electron microscopic observation of the complexes showed a kinked configuration of the ternary complexes. Statistic analysis of the observed configuration demonstrated the existence of various species of the S1·ADP·BeFn complex. These results suggest that the ternary complexes mimic the different structures of transient intermediates in the ATPase cycle distributing from M^{*}·ATP to M^{**}·ADP·Pi.

This work was supported by Grants in Aid for Scientific Research C (11680667), for Scientific Research B and, for Scientific Research on Priority Areas from the Ministry of Education, Science, Sports and Culture of Japan.

REFERENCES

1. Johnson, W.C., Jr., Bivin, D.B., Ue, K., and Morales, M.F. (1991) A search for protein structural changes accompanying the contractile interaction. *Proc. Natl. Acad. Sci. USA* **88**, 9748–9750
2. Hiratsuka, T. (1992) Spatial proximity of ATP-sensitive tryptophanyl residue(s) and Cys-697 in myosin ATPase. *J. Biol. Chem.* **267**, 14949–14954
3. Park, S., Ajtai, K., and Burghardt, T.P. (1996) Optical activity of a nucleotide-sensitive tryptophan in myosin subfragment 1 during ATP hydrolysis. *Biophys. Chem.* **63**, 67–80
4. Cheung, H.C., Gryczynski, I., Malac, H., Wiczk, W., Johnson, M.L., and Lakowicz, J.R. (1991) Conformational flexibility of the Cys 697–Cys 707 segment of myosin subfragment-1. Distance distributions by frequency-domain fluorometry. *Biophys. Chem.* **40**, 1–17
5. Reisler, E., Burke, M., Himmelfarb, S., and Harrington, W.F. (1974) Spatial proximity of the two essential sulfhydryl groups of myosin. *Biochemistry* **13**, 3837–3840
6. Wells, J.A. and Yount, R.G. (1982) Chemical modification of myosin by active-site trapping of metal-nucleotides with thiol crosslinking reagents. *Methods Enzymol.* **85**, 93–116
7. Miyanishi, T., Inoue, A., and Tonomura, Y. (1979) Differential modification of specific lysine residues in the two kinds of subfragment-1 of myosin with 2, 4, 6-trinitrobenzenesulfonate. *J. Biochem.* **85**, 747–753
8. Komatsu, H., Emoto, Y., and Tawada, K. (1993) Half-stoichiometric trinitrophenylation of myosin subfragment 1 in the presence of pyrophosphate or adenosine diphosphate. *J. Biol. Chem.* **268**, 7799–7808
9. Mornet, D., Pantel, P., Bertrand, R., Audemard, E., and Kassab, R. (1980) Localization of the reactive trinitrophenylated lysyl residue of myosin ATPase site in the NH_2-terminal (27 k domain) of S1 heavy chain. *FEBS Lett.* **17**, 183–188
10. Wakabayashi, K., Tokunaga, M., Kohno, I., Sugimoto, Y., Hamanaka, T., Takezawa, Y., Wakabayashi, T., and Amemiya, Y. (1992) Small-angle synchrotron x-ray scattering reveals distinct shape changes of the myosin head during hydrolysis of ATP. *Science* **258**, 443–447
11. Sugimoto, Y., Tokunaga, M., Takezawa, Y., Ikebe, M., and Wakabayashi, K. (1995) Conformational changes of the myosin head during hydrolysis of ATP as analyzed by x-ray solution scattering. *Biophys. J.* **68**, 29s–34s
12. Maruta, S., Henry, G.D., Sykes, B.D., and Ikebe, M. (1993) Formation of the stable myosin-ADP-aluminum fluoride and myosin-ADP-beryllium fluoride complex and their analysis using ^{19}F-NMR. *J. Biol. Chem.* **268**, 7093–7100
13. Werber, M.M., Peyser, Y.M., and Muhlrad, A. (1992) Characterization of stable beryllium fluoride, aluminum fluoride, and vanadate containing myosin subfragment 1-nucleotide complexes. *Biochemistry* **31**, 7190–7197
14. Phan, B. and Reisler, E. (1992) Inhibition of myosin ATPase by beryllium fluoride. *Biochemistry* **31**, 4787–4793
15. Goodno, C.C. (1979) Inhibition of myosin ATPase by vanadate ion. *Proc. Natl. Acad. Sci. USA* **76**, 2620–2624
16. Gopal, D. and Burke, M. (1995) Formation of stable inhibitory complexes of myosin subfragment 1 using fluoroscandium anions. *J. Biol. Chem.* **270**, 19282–19286
17. Smith, C.A. and Rayment, I. (1995) X-ray structure of the magnesium (II)-pyrophosphate complex of the truncated head of *Dictyostelium discoideum* myosin to 2.7 Å resolution. *Biochemistry* **34**, 8973–8981
18. Fisher, A.J., Smith, C.A., Thoden, J.B., Smith, R., Sutoh, K., Holden, H.M., and Rayment, I. (1995) X-ray structures of the myosin motor domain of *Dictyostelium discoideum* complexed with MgADP·BeFx and MgADP·AlF_4^-. *Biochemistry* **34**, 8960–8972
19. Smith, C.A. and Rayment, I. (1996) X-ray structure of the magnesium (II). ADP·vanadate complex of the *Dictyostelium discoideum* myosin motor domain to 1.9 Å resolution. *Biochemistry* **35**, 5404–5417
20. Rayment, I., Rypniewski, W.R., Schmidt-Bäse, K., Smith, R., Tomchick, D., Benning, M.M., Winkelman, D.A., Wesenberg, G., and Holden, H.M. (1993) Three-dimensional structure of myosin subfragment-1: a molecular motor. *Science* **261**, 50–58
21. Maruta, S., Uyehara, Y., Homma, K., Sugimoto, Y., and Wakabayashi, K. (1999) Formation of the myosin.ADP.gallium

fluoride complex and its solution structure by small-angle synchrotron x-ray scattering. *J. Biochem.* **125**, 177–185
22. Dominquez, R., Freyzon, Y., Trybus, K.M., and Cohen, K. (1998) Crystal structure of a vertebrate smooth muscle myosin motor domain and its complex with the essential light chain: visualization of the pre-power stroke state. *Cell* **94**, 559–571
23. Houdusse, A., Kalabokis, V., N., Himmel, D., SzentGyorgy, A.G., and Cohen, C. (1999) Atomic structure of scallop myosin subfragment S1 complexed with MgADP: A novel conformation of the myosin head. *Cell* **97**, 459–470
24. Houdusse, A., SzentGyorgy, A.G., and Cohen, C. (2000) Three conformational states of scallop myosin S1. *Proc. Natl Acad. Sci. USA.* **97**, 11238–11243
25. Macgregor, R.B. and Weber, G. (1986) Estimation of the polarity of the protein interior by optical spectroscopy. *Nature* **319**, 70–73
26. Mazumdar, M., Parrack, P.K., and Bhattacharyya, B. (1992) Interaction of prodan with tubulin. A fluorescence spectroscopic study. *Eur. J. Biochem.* **204**, 127–132
27. Chakrabarti, A. (1996) Fluorescence of spectrin-bound prodan. *Biochem. Biophys. Res. Commun.* **226**, 495–497
28. Hiratsuka, T. (1998) Prodan fluorescence reflects differences in nucleotide-induced conformational states in the myosin head and allows continuous visualization of the ATPase reactions. *Biochemistry* **37**, 7167–7176
29. Heuser, J.E. (1983) Procedure for freeze-drying molecules adsorbed to mica flakes. *J. Mol. Biol.* **169**, 155–195
30. Katayama, E. (1998) Quick-freeze deep-etch electron microscopy of the actin-heavy meromyosin complex during the in vitro motility assay. *J. Mol. Biol.* **278**, 349–367
31. Perry, S.V. (1952) Myosin adenosine triphosphatase. *Methods Enzymol.* **2**, 582–588
32. Weeds, A.G. and Taylor, R.S. (1975) Separation of subfragment-1 isoenzymes from rabbit skeletal muscle myosin. *Nature* **257**, 54–56
33. Weeds, A.G. and Pope, B. (1977) Studies on the chymotryptic digestion of myosin. Effects of divalent cations on proteolytic susceptibility. *J. Mol. Biol.* **111**, 129–57
34. Heuser, J.E., Reese, T.S., Dennis, M.J., Jan, Y., Jan, L., and Evans, L. (1979) Synaptic vesicle oxocytosis captured by quick freezing and correlated with quantal transmitter release. *J. Cell Biol.* **81**, 275–300
35. Park, S., Ajtai, K., and Burghardt, T.P. (1999) Inhibition of myosin ATPase by metal fluoride complexes. *Biochim. Biophys. Acta* **1430**, 127–1240
36. Phan, B.C., Cheung, P., Stafford, W.F., and Reisler, E. (1996) Complexes of myosin subfragment-1 with adenosine diphosphate and phosphate analogs: probes of active site and protein conformation, *Biophys. Chem.* **59**, 341–349
37. Phan, B.C., Peyser, Y.M., Reisler, E., and Muhlrad, A. (1997) Effect of complexes of ADP and phosphate analogs on the conformation of the Cys707–Cys697 region of myosin subfragment-1, *Eur. J. Biochem.* **243**, 636–642
38. Henry, G.D., Maruta, S., Ikebe, M., and Sykes, B.D. (1993) Observation of Multiple myosin subfragment-1:ADP:fluoroberyllate complexes by ^{19}F-NMR, *Biochemistry* **32**, 10451–10456
39. Maruta, S., Henry, G.D., Sykes, B.D., and Ikebe, M. (1998) Analysis of stress in the active site of myosin accompanied by conformational changes in transient state intermediate complexes using photoaffinity labeling and ^{19}F-NMR spectroscopy. *Eur. J. Biochem.* **252**, 520–529